

## SOLAR-TO-HYDROGEN PHOTOVOLTAIC/PHOTOELECTROCHEMICAL DEVICES USING AMORPHOUS SILICON CARBIDE AS THE PHOTOELECTRODE

Jian Hu<sup>a</sup>, Feng Zhu<sup>a,b</sup>, Ilvydas Matulionis<sup>a</sup>, Augusto Kunrath<sup>a</sup>, Todd Deutsch<sup>c</sup>, Eric Miller<sup>d</sup>, and Arun Madan<sup>a,b</sup>

a: MVSystems, Inc., 500 Corporate Circle, Suite L, Golden, CO, 80401, USA.

b: Department of Physics, Colorado School of Mines, Golden, CO 80401, USA.

c: National Renewable Energy Laboratory, Golden, CO 80401, USA.

d: Hawaii Natural Energy Institute, University of Hawaii at Manoa, Honolulu, HI 96822, USA.

**ABSTRACT:** We report the use of hydrogenated amorphous silicon carbide (a-SiC:H) prepared by plasma enhanced chemical vapor deposition (PECVD) as the photoelectrode in an integrated “hybrid” photoelectrochemical (PEC) cell to produce hydrogen directly from water using sunlight. Results on the durability of hydrogenated amorphous silicon carbide (a-SiC:H) photoelectrodes in an electrolyte are presented. In a pH2 electrolyte, the a-SiC:H photoelectrode exhibits excellent stability for 100 hour test so far performed. A photocurrent onset shift (anodically) after a 24- or 100-hour durability test in electrolyte is observed, likely due to changes in the surface chemical structure of the a-SiC:H photoelectrode. It is also observed that a thin SiO<sub>x</sub> layer native to the air exposed surface of the a-SiC:H affects the photocurrent and the its onset shift. Finally, approaches for eliminating the external bias voltage and enhancing the solar-to-hydrogen efficiency in a PV/PEC hybrid structure to achieve  $\geq 10\%$  are presented.

**Keywords:** Amorphous silicon carbide, Hydrogen, PECVD

### 1. Introduction

Hydrogen is emerging as an alternative energy carrier to fossil fuels due to its non-toxic and environmentally friendly nature. To obtain hydrogen, it must be extracted from various sources, which requires energy. While a hydrogen-oxygen fuel cell operates without generating emission, hydrogen production through conventional means (e.g., direct electrolysis, steam-methane reformation, thermo-chemical decomposition of water and so on) can give rise to significant greenhouse gases and other harmful byproducts. Compared with other methods, photoelectrochemical (PEC) water splitting at a semiconductor-electrolyte interface using sunlight is of considerable interest as it offers an environmentally “green” approach to hydrogen production [1,2]. Efficient PEC water splitting devices require photoelectrode semiconductor materials fulfilling a number of primary requirements, such as bandgap ( $E_g$ ), band edge alignment, corrosion resistance to electrolyte etc. We have previously reported on a multi-junction PEC device with amorphous silicon photovoltaic junctions and a WO<sub>3</sub> photoanode, leading to a 3% solar-to-hydrogen (STH) efficiency [3] and a similar PEC device with hydrogenated amorphous silicon carbide (a-SiC:H) photoelectrodes fabricated by the PECVD technique [4]. A schematic diagram of an integrated PV/PEC hybrid device of this kind for water splitting is shown in Fig.1. Compared with conventional large bandgap photoelectrode materials (e.g., WO<sub>3</sub> with  $E_g$  of  $\sim 2.8$ eV), a-SiC:H films with a lower  $E_g$  (2.0-2.3eV) would absorb

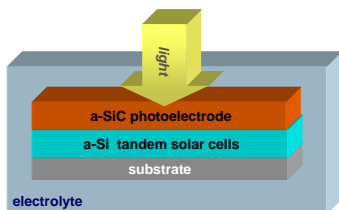
Fig.1 Integrated PV/PEC hybrid device used for water splitting to generate hydrogen.

more photons from sunlight, and thus should enhance the STH conversion efficiency. It should be noted that a-SiC:H films are used routinely as a window (p<sup>+</sup>) layer in a-Si solar cells as its  $E_g$  can be increased to  $\sim 2$  eV with C incorporation. In addition, incorporation of the C in the film should lead to an increase in the corrosion resistance compared to the use of conventional a-Si:H films, which have poor stability in the electrolyte [5]. Moreover, a-SiC:H films are routinely prepared by the PECVD technique which is normally used in the fabrication of a-Si tandem solar cells. This could become very attractive for mass-production of PEC devices in a cost-effective fashion.

In this paper, we focus on the study of the a-SiC:H used as the photoelectrode, including improved durability and photocurrent generation in an electrolyte. We will also discuss the roadmap to achieve STH  $> 10\%$  using an integrated PV/PEC hybrid device.

### 2 Experimental details

A-SiC:H films were fabricated in a PECVD cluster tool system specifically designed for the thin film semiconductor market and manufactured by MVSystems, Inc. The intrinsic a-SiC:H films were deposited using H<sub>2</sub>, CH<sub>4</sub> and SiH<sub>4</sub> gas mixtures at 200°C. The flow rates were varied from 0 to 12 sccm for CH<sub>4</sub>. During the deposition, the pressure was kept at 400-900 mTorr and the RF power density used was in the range of 8-20 mW/cm<sup>2</sup>. For a-SiC:H p-i-n solar cells, the p-layer was a-SiC:H:B and was deposited from SiH<sub>4</sub>, CH<sub>4</sub>, and B<sub>2</sub>H<sub>6</sub> gas mixtures while the n-layer was prepared using SiH<sub>4</sub> and PH<sub>3</sub> gas mixture. The basic optoelectronic properties of a-SiC:H films such as dark and photoconductivity,  $\gamma$  factor (deduced from the photocurrent ( $I_{ph}$ ) vs. light intensity (F) plot,  $I_{ph} \propto F^\gamma$ ), and the solar cell performance such as the short-circuit current ( $J_{sc}$ ), open-circuit voltage ( $V_{oc}$ ), fill-factor (FF) and efficiency, were



characterized by an in-house J-V station with a calibrated Global AM 1.5 light source (Xenon lamp). The spectral response (quantum efficiency) of solar cells was measured with narrow bandwidth filters.  $E_g$  was deduced using Tauc's plot. Si-H and Si-C bonding configurations in a-SiC:H films were determined by infrared (IR) spectroscopy data.

The configuration used for the a-SiC:H photoelectrode is shown in Fig.2 and consists of an intrinsic a-SiC:H (~200 nm thick) and a thin p-type a-SiC:H:B layer (~20 nm thick). In general, the a-SiC:H

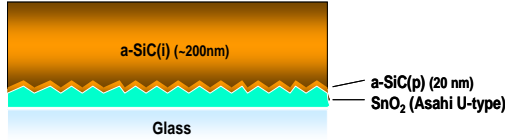


Fig.2. Configuration of a-SiC photoelectrodes.

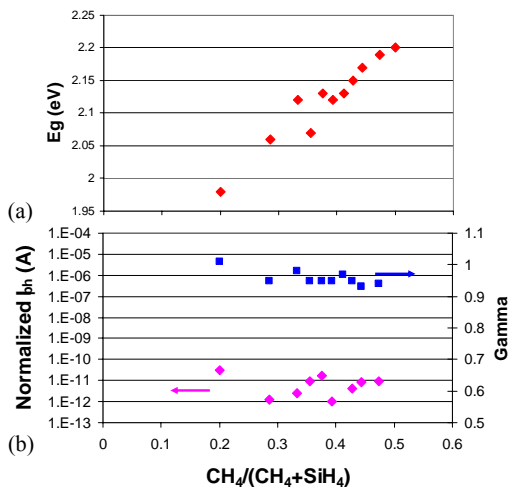
photoelectrode behaves like a photocathode where the photogenerated electrons inject into the electrolyte at the a-SiC(i)/electrolyte interface to reduce  $H^+$  ions for hydrogen evolution. This way, anodic reactions and thus corrosion on a-SiC:H layer can be mitigated.

PEC properties of the a-SiC:H photoelectrodes were evaluated at the National Renewable Energy Laboratory (NREL) and the Hawaii Natural Energy Institute (HNEI) using three- and two-electrode setups.

### 3. Results and Discussion

#### 3.1 a-SiC:H material

Fig.3(a) shows  $E_g$  of a-SiC:H materials as a



function of the gas ratio  $CH_4/(CH_4+SiH_4)$  used during the Fig.3. (a)  $E_g$  vs.  $CH_4/(CH_4+SiH_4)$ ; (b) Normalized photocurrent ( $I_{ph}$ ) and Gamma ( $\gamma$ ) vs.  $CH_4/(CH_4+SiH_4)$ .

growth. As this gas ratio increases from 0.2 to ~0.5,  $E_g$  increases nearly linearly from 1.98 eV to ~2.2 eV, due to increasing C incorporation. Typically for a-SiC:H films with  $E_g=2$  eV, the C concentration, as determined by X-ray photoelectron spectroscopy (XPS), is ~7%. It should

be noted from Fig.3(b) that as  $E_g$  increases to ~2.2 eV, the  $\gamma$  factor, from which we infer the DOS (density of defect states) of the amorphous semiconductor [6], only decreases slightly, from ~1 to 0.94, indicating little change in the defect density in the films. We also note that the photocurrent ( $I_{ph}$ ), which is normalized by taking into account changes of the absorption coefficient with  $E_g$ , does not show a significant change as  $E_g$  increases. This then suggests that the DOS has remained low and is consistent with  $\gamma \sim 1$  (low DOS) throughout the range and up to  $E_g \sim 2.2$  eV.

#### 3.2 Solar cells using a-SiC:H material as the absorber

The previous results suggest that high quality a-SiC:H materials can be fabricated with  $E_g$  of 2.0-2.2 eV. To test the viability of the material in a junction, we have incorporated the material into p-i-n structure and constructed as normal solar cells in the configuration, glass/Asahi U-Type  $SnO_2/p$ -a-SiC:B:H/i-a-SiC:H/n-a-Si/Ag. The Ag top contact defines the device area as to be  $0.25 \text{ cm}^2$ . The thickness of the i-layer is ~300 nm. Fig.4 shows the J-V curve under Global AM1.5

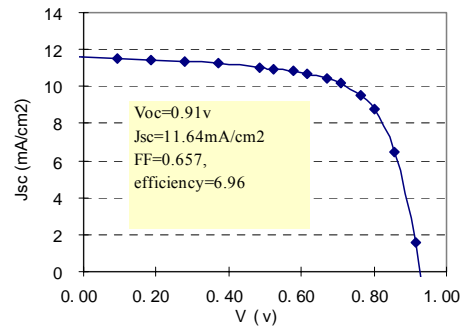


Fig.4. The light current-voltage characteristic of a-SiC:H solar cell.

illumination. It is seen that  $V_{oc} = 0.91 \text{ V}$ ,  $J_{sc} = 11.64 \text{ mA/cm}^2$ ,  $FF = 0.657$ ;  $FF$  under blue (400 nm) illumination and  $FF$  under red (600 nm) illumination both exhibit 0.7. At reduced a-SiC:H intrinsic layer thickness of ~100 nm,  $J_{sc}$  of ~8.45  $\text{mA/cm}^2$  has been obtained. This data is very close to the previously reported a-SiC:H solar cell [7].

#### 3.3 Durability of a-SiC:H photoelectrodes

Four types of substrates with different surface texture or roughness were chosen for durability tests. All samples had the same structure as shown in Fig.2 with the substrates being: (1) glass/ $SnO_2:F$  (textured), (2) glass/ $ZnO$  (specular), (3) 0.7 mm thick polished stainless steel (SS) and (4) 0.7 mm thick polished stainless steel with a 300 nm film of molybdenum (SS/Mo). The electrolyte used was pH2 sulphamic acid/potassium biphthalate solution and a Triton X-100 surfactant. During testing, a constant current density of  $-3 \text{ mA/cm}^2$  was applied to the a-SiC:H photoelectrode. These samples were illuminated with a tungsten lamp (calibrated to Global AM1.5 intensity with a 1.8eV reference cell). After a 24-hour test, it was found that the a-SiC:H photoelectrode on glass/ $SnO_2:F$  and glass/ $ZnO$  remained largely intact. The durability of the a-SiC:H photoelectrodes on glass/ $SnO_2:F$  was then tested by

further extending the test period to 100 hours. The good durability of a-SiC:H photoelectrodes was confirmed by the chopped light current-voltage characteristics which was measured before and after the 100 test and is shown in Fig.5. It is seen that the dark current of both photoelectrodes (#1 and #2) remains unchanged, indicative of no corrosion.

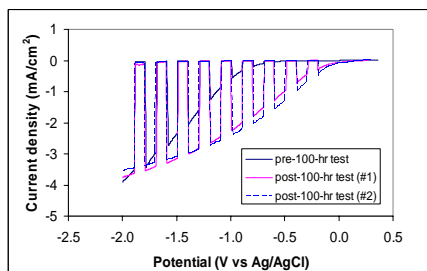


Fig.5. Current density vs. potential characteristics measured with three-electrode configuration.

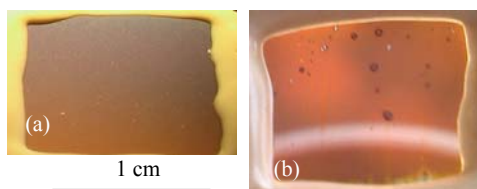


Fig. 6. a-SiC:H film on glass/SnO<sub>2</sub>:F substrate (a) before and (b) after a 100-hour test. (During the photo the film (a) was front illuminated and (b) was back lit).

Interestingly, as shown in Fig. 6, we noted that morphology of the a-SiC:H photoelectrode remains unchanged except for a few localized blemishes, whose nature is not completely clear. It should be emphasized that the blemishes may be merely cosmetic as the I-V curve before and after the 100 hour test changes little, as seen in Fig. 5. Further analysis of these spots using the Energy Dispersive X-ray Spectroscopy (EDS) is currently underway.

### 3.4 Photocurrent onset shift

It is interesting to note from Fig.5 that, after the 100-hr durability test, the photocurrent (PC) onset shifts anodically, or towards the low bias regime and the device actually improves. This behavior was found to be repeatable, for instance, both the sample of type #1 and #2 show almost identical PC onset shift. In addition, the PC onset shift became even more pronounced as the testing duration time was increased from 24 hours to 100 hours. However, the PC degrades gradually when the a-SiC:H photoelectrode is re-exposed to air for up to two months, as shown in Fig.7 and is probably due to surface oxidation. In order to test this theory, we performed a hydrofluoric acid (HF) etch experiment. The as-prepared a-SiC:H photoelectrodes were measured, dipped in HF for 10-30 secs, and then measured again. Fig.8 shows a comparison of the current density vs. voltage characteristics measured before (dark curve) and after (pink curve) the HF dip. It is seen that after the HF dip, photocurrent increases noticeably, e.g., from 2.92 mA/cm<sup>2</sup>

to 6.3 mA/cm<sup>2</sup> at -1.4 V (vs. Ag/AgCl). Meanwhile, the photocurrent onset shifts anodically by about 0.23 V. Interestingly, after the a-SiC:H photoelectrode was

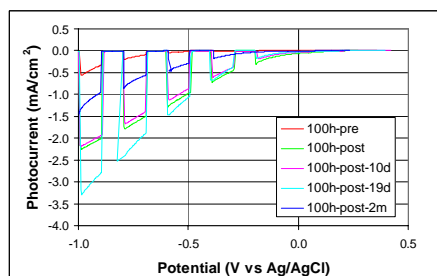


Fig.7. Current density -potential characteristics measured in cases of before and after a 100-hour durability test, and then 10 days through 2 months later.

removed from the electrolyte and exposed to air for 67 hours, the photocurrent degrades and completely returns to its original value (as shown by

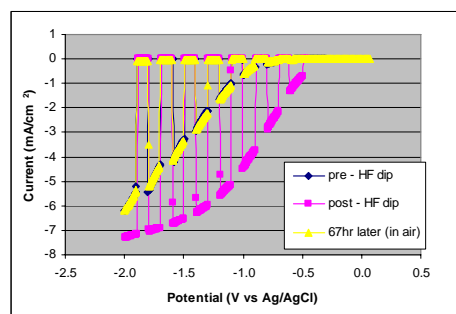


Fig.8. Effect of the thin SiO<sub>x</sub> on photocurrent. Dark curve - pre-HF dip; Pink curve - post-HF dip; and yellow curve -in the air for 67 hours after the HF dip.

the yellow curve). This result confirms that decrease of PC in the air is caused by the formation of the SiO<sub>x</sub> layer on the surface of the a-SiC:H photoelectrode. The XPS analysis also confirmed that after the HF dip for 30 secs, the Si-O bonds almost disappeared at the a-SiC:H surface [8].

### 3.5 Flatband potential

Fig.9 shows the illuminated open-circuit potential (OCP) as a function of pH of electrolyte for a-SiC:H photoelectrodes on SS, SS/Mo and SnO<sub>2</sub> substrates. The

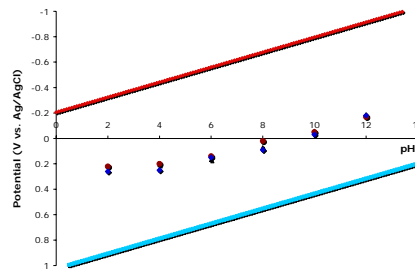


Fig.9. The illuminated open-circuit potential (OCP) vs. pH.

OCP vs. pH nearly follows a correlation of  $\sim 60$  mV/pH, as predicted by the Nernst equation [9]. It is also seen that at pH=2, the flatband voltage ( $\approx$ OCP) = +0.26V (vs. Ag/AgCl), which is above the  $H_2O/O_2$  redox potential by about 0.7 V. Based on this measured flatband potential and the photovoltage data, the energy band diagram for the a-SiC(p)/a-SiC(i)/Electrolyte system under illumination and an external bias is shown in Fig.10.

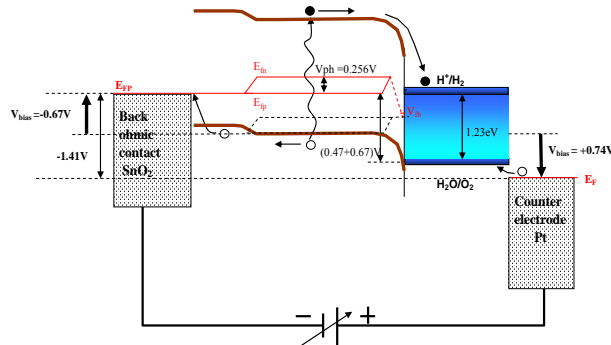


Fig.10. The schematic energy diagram for the a-SiC(p)/a-SiC(i)/Electrolyte system under illumination and external biases.

It can be seen quite clearly that the hydrogen evolution reaction is unrestricted at the surface of the a-SiC:H photoelectrode, since the photogenerated electrons are injected into the solution at a higher (more negative) potential than the redox potential of  $H^+/H_2$ . On the other hand, to promote oxygen evolution at the counter electrode (Pt), a minimum external bias of  $\sim -1.4$  V is needed to bring the quasi-Fermi energy level of photogenerated holes,  $E_{Fp}$  below  $H_2O/O_2$  redox potential.

#### 4. Solar-to-hydrogen efficiency >10% - roadmap

According to the U.S. Department of Energy, the technical objective defined for the PEC Hydrogen Production using Silicon-based compound films photoelectrodes requires a STH efficiency  $\sim 5\%$  for the near-term (by 2009) and 10% by 2018 [10]. In order to reach these goal, we will integrate an a-Si tandem solar cell with the a-SiC:H photoelectrode, since the PV/PEC hybrid structure (see Fig. 11) will provide the needed voltage (sum of  $V_{ph1} + V_{ph2} + V_{ph3}$ )  $> 2$  V for water splitting. The photocurrent should reach 4-5 mA/cm<sup>2</sup>, or a STH efficiency  $\geq 5\%$ .

Further enhancement in the STH efficiency could be achieved by employing a nano-crystalline (nc) Si

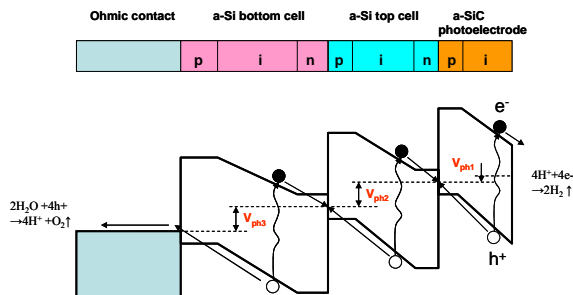


Fig.11. The schematic energy band diagram of a hybrid PV/PEC cell containing a-SiC photoelectrode and a-Si/a-Si tandem solar cells.

p-i-n solar cell (used as the bottom cell) in the tandem solar cell, integrated with the a-SiC:H photoelectrode as shown in Fig.11. We expect that with such a configuration, a photocurrent of  $\sim 8$  mA/cm<sup>2</sup> would be generated, leading to a STH efficiency up to  $\sim 10\%$ .

#### 5. Conclusion

We have fabricated good-quality a-SiC:H photoelectrodes in PEC cell configuration for hydrogen production directly from water using sunlight. We have so far tested the durability of this photoelectrode in a pH2 electrolyte for 100 hours. During this time frame PC onset shifts towards a low bias, possibly due to changes in the surface structure of the a-SiC:H photoelectrode. The HF etch experiment shows that the surface SiOx layer affects the PC and the PC onset shift.

#### Acknowledgement

The authors would like to thank Ed Valentich for his assistance in sample fabrication, Leah Kuritzky of National Renewable Energy Laboratory for various PEC characterization, and Marcus Baer and Clemens Heske of University of Nevada at Las Vegas for XPS measurements. We would also like to thank John Turner of National Renewable Energy Laboratory for many helpful discussions.

The work is supported by US Department of Energy under contract number DE-FC36-07GO17105.

#### 6. References

- [1] T. Ohta, "Solar-Hydrogen Energy Systems", Pergamon Press, 1979.
- [2] R. Narayanan and B. Viswanathan, "Chemical and Electrochemical Energy Systems", University Press (India), 1998.
- [3] A. Stavrides, A. Kunrath, J. Hu, R. Treglio, A. Feldman, B. Marsen, B. Cole, E.L. Miller, and A. Madan, Proc. SPIE, Vol. 6340, (2006)63400K.
- [4] F. Zhu, J. Hu, A. Kunrath, I. Matulionis, B. Marsen, B. Cole, E.L. Miller, and A. Madan, Proc. SPIE, Vol. 6650, (2007)66500S.
- [5] K. Varner, S. Warren and J. A. Turner, Proceedings of the 2002 U.S. DOE Hydrogen Program Review, NREL/CP-610-32405.
- [6] A. Madan and M.P. Shaw, "The Physics and Applications of Amorphous Semiconductors", Academic Press, 1988, p. 99.
- [7] R.E.Hollingsworth, P.K.Bhat, and A.Madan, Proc. 19th IEEE PVSC, 1987, p. 684.
- [8] M. Baer and C. Heske, Interim report, DOE PEC Workshop, Santa Barbara, January, 2008.
- [9] R. Memming, "Semiconductor Electrochemistry", Wiley-VCH, 2001.
- [10] Statement of Project Objectives, US Department of Energy, #DE-FC36-07GO17105; See also R. Garland et al, DOE Hydrogen Production Review Meeting, Arlington, VA, June 12, 2008.